

Fig. 1 Thermocouple spectra for two different thermocouples placed on the centerline at the exhaust plane of a gas turbine combustor.

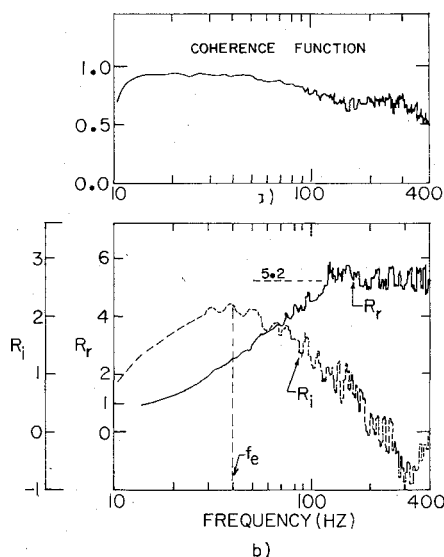


Fig. 2 Coherence a) between the two thermocouples and b) time constant determination for the thermocouples.

markedly at high frequency there is much more danger of dropping into the background noise at high frequency as compared with  $\omega_e$ .

### Experiment

To illustrate the procedure two commercial Chromel-Alumel thermocouples of wire diameters 0.001 in. (TC1) and 0.003 in. (TC2) were mounted less than 1/8 in. apart in the exhaust of a gas turbine combustor. Fixed bandwidth spectra (15.6 Hz) of the AC component of temperature are shown in Fig. 1. Also shown in Fig. 1 is the true temperature spectrum ( $\eta^2 X_i X_i^*$ ) after correction, knowing the thermocouple time constant. Since the time constant goes roughly as  $D^{1.5}$ , where  $D$  is the wire diameter, TC2 has a poorer response, which is also shown in Fig. 1. In this example the ratio of the time constant,  $\tau_2/\tau_1$ , should be roughly  $3^{1.5} = 5.2$ .

The time constant for TC1 was expected to lie between 1 and 10 msec, so finer bandwidth filtering (3.1 Hz), and a narrower frequency range (0-400 Hz) was chosen for time constant analysis in Fig. 2. In Fig. 2a, the coherence function is seen to be adequate within the band 10-400 Hz. In Fig. 2b are shown  $R_r$  and  $R_i$ .  $R_r$  shows the expected behavior of monotonically going from unity to  $\tau_2/\tau_1$  as  $\omega$  goes from zero to values much greater than  $1/\tau_1$ .  $R_i$  shows the expected behavior of a maximum at 40 Hz, corresponding to  $\tau_1 = 1/(2\pi 40) = 4$  msec.

Some problems with this method are a) the AC component of temperature is usually substantially lower than the DC component so that high systems gains are needed and higher than desired background noise is usually evident, especially for the larger thermocouple, and b) the maximum is somewhat broad in  $R_i$  so that, in this example, about 25% error in  $\tau$  may be expected. Problem a) is minimized by using thermocouples of nearly equivalent (but not equal) time constants. However, it appears that problem b) must be accepted as a limitation of the method.

### References

- <sup>1</sup>Zukoski, E., "Temperature Distortion Effect on Turbine and Afterburner Noise," ASME Paper No. 75-6T-40, 1975.
- <sup>2</sup>Cumpsty, N. A., "Excess Noise from Gas Turbine Exhausts," ASME Paper No. 75-6T-61, 1975.
- <sup>3</sup>Pickett, G. F., "Core Engine Noise due to Temperature Fluctuations Convecting through Turbine Blade Rows," AIAA Paper 75-528, Hampton, Va., 1975.
- <sup>4</sup>Scadron, M. D. and Warshawsky, S., "Experimental Determination of Time Constants and Nusselt Numbers for Bare-Wire Thermocouples in High-Velocity Air Streams and Analytic Approximation of Conduction and Radiation Errors," NACA TN 2599, 1952.
- <sup>5</sup>Carbon, M. W., Kutsch, H. J., and Hawkins, G. A., "The Response of Thermocouples to Rapid Gas-Temperature Changes," ASME Transactions, July 1950, pp. 655-657.
- <sup>6</sup>Bendat, J. S. and Piersol, A. G., *Random Data: Analysis and Measurement Procedures*, Wiley-Interscience, N. Y., 1975, p. 32.

## Preheated, Combustion-Driven Gasdynamic Lasers

R. C. Saunders III\* and L. J. Otten III\*

NASA Ames Research Center, Moffett Field, Calif.

### Introduction

EARLY in the development of the carbon dioxide gasdynamic laser (GDL), the variation in available laser energy as a function of laser gas stagnation temperature was readily noticeable. Experiments performed on a variety of laboratory devices<sup>1,2</sup> suggested that the laser energy available in a given device would be improved by operating with stagnation temperatures in the region of 2100 K, that is, at temperatures considerably above those of then-current devices. These experiments were generally performed on shock tube or arc-driven GDLs and, therefore, the gas composition was independent of any combustion process. For many applications, however, shock tube or arc-driven devices are not adequate. A solution is to use a combustion-driven device (first demonstrated by workers at AVCO Everett Research Laboratory<sup>3</sup>) in which reactants are burned to produce the necessary high-temperature laser gas. The disadvantage to this solution is that laser gas composition and stagnation temperature are no longer independent. In obtaining the higher temperatures necessary for more efficient operation, one encounters either undesirable laser gas compositions (which tend to negate the effect of the increased temperature) or fuel-oxidizer combinations that are not very practicable.

One method of eliminating the dependence of laser gas composition and temperature while still maintaining a

Received Jan. 20, 1976; presented as Paper 76-58 at the AIAA 14th Aerospace Sciences Meeting, Washington, D.C., Jan. 26-28, 1976; revision received May 3, 1976.

Index category: Lasers.

\*Air Force Systems Command Laboratory Associate. Member AIAA.

Table 1 GDL characteristics

Nozzle area ratio	Nozzle throat height (mm)	Stagnation temperature ( $^{\circ}$ K)	Stagnation pressure (atm)	$\psi_{\text{CO}_2}$ (molar)	$\psi_{\text{H}_2\text{O}}$ (molar)	$\psi_{\text{He}}$ (molar)	Fuel/oxidizer
			30				
56	0.165	1338	45	0.10	0.005	0.022	CO/N <sub>2</sub> O
			54				
			62				

workable fuel-oxidizer combination is to preheat the nitrogen that is added to the combusted gases. This technique, while not new, has not been widely utilized.

In the work reported here, the effect of preheated nitrogen on the available specific energy for an advanced combustion-driven gasdynamic laser is described. This theoretical analysis combined a nonequilibrium model of the relevant GDL processes with a simplified, nondissociating combustion model capable of handling a variety of candidate GDL fuels. The GDL model is described in detail in Ref. 4. The combustion model employs an energy and mass balance approach to determine the flame temperature and gas composition.<sup>5</sup> A variable initial reactant temperature is used to describe the preheating. To explore more fully the possibilities of preheating, an optimization routine<sup>6</sup> was added to the combined laser/combustion models. The use of this technique permitted the selection of optimum laser operating characteristics at any level of preheating.

### Results

The laser that was examined is representative of a second generation of gasdynamic lasers. These devices are characterized by higher temperatures, pressure, and nozzle area ratios than the earlier generation devices. The laser used in this analysis is based on the lasers described in Refs. 2, 7, and 8. Its characteristics and nominal operating features are listed in Table 1, where  $\psi_{\text{CO}_2}$ ,  $\psi_{\text{H}_2\text{O}}$ , and  $\psi_{\text{He}}$  are the laser gas molar concentrations of CO<sub>2</sub>, H<sub>2</sub>O, and He, respectively. The use of various stagnation pressures was suggested by the stagnation pressure effects found in Ref. 7.

Table 2 summarizes the predicted performance of this laser with and without preheating. No optimization was used. The available specific energy  $\epsilon$ , averaged over a 10 cm downstream distance where it was largest, was chosen as the figure of merit. Small signal gain  $g_0$ , important for extraction considerations, was also checked at selected points to insure that it was large enough to allow efficient power extraction, i.e.,  $g_0 \geq 1\%/cm$ .  $\Delta T$  is the nitrogen temperature increase above room temperature due to preheating, and  $T_0$  is the total gas stagnation temperature due to combustion plus preheating. Cooling losses are neglected.  $P_0$  is the gas stagnation pressure. The gas composition used is given in Table 1.

The optimization routine was then used at each  $\Delta T$  to select the combination of the laser operating parameters that would maximize the available specific energy. Two design variables were employed in these optimizations: water concentrations and the ratio of nitrogen to fuel which determines CO<sub>2</sub> concentration and stagnation temperature. The objective function was the average available specific energy. To avoid the region of dissociation for CO<sub>2</sub>, a stagnation temperature constraint of 2100 K was imposed. Although the optimization procedure is sufficiently general to handle a large number of laser design parameters, nozzle geometry, stagnation pressure, helium concentration, and the fuel/oxidizer of Table 1 were used as fixed values in order to isolate the preheating effect.

Table 3 presents the results of optimizing the laser with and without preheating. The results of Table 2 are presented for

Table 2 GDL performance results (nonoptimal)

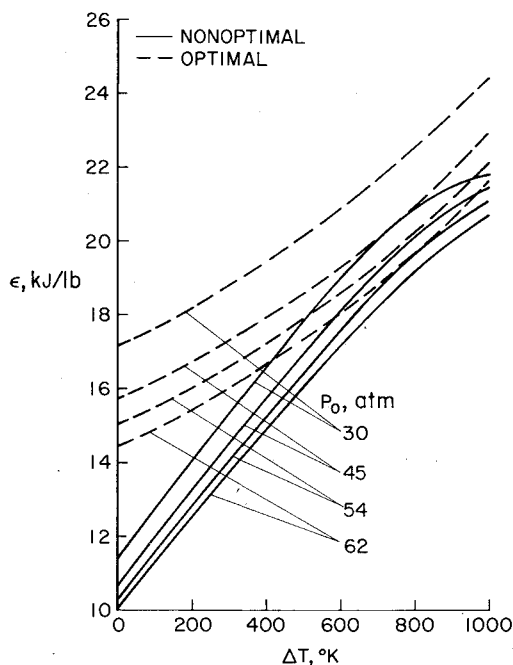
$P_0$ , atm	$\Delta T$ , $^{\circ}$ K	$T_0$ , $^{\circ}$ K	$\epsilon$ , kJ/lb
30	0	1338	11.4
	250	1491	14.7
	500	1646	17.8
	750	1811	20.5
	1000	1980	21.8
45	0	1338	10.7
	250	1491	13.9
	500	1646	16.9
	750	1811	19.6
	1000	1980	21.5
54	0	1338	10.4
	250	1491	13.4
	500	1646	16.4
	750	1811	19.2
	1000	1980	21.1
62	0	1338	10.1
	250	1491	13.1
	500	1646	16.0
	750	1811	18.7
	1000	1980	20.7

comparison. Note that in all cases a higher specific energy has been obtained. Note too that the operating parameters are different for each of the lasers. The optimizer has selected the best combination of the design variables to maximize  $\epsilon$  for that particular laser.

Figure 1 compares the performance of the lasers at varying amounts of preheating. For the nonoptimized lasers, the available specific energy increases as the nitrogen temperature increases, but at high nitrogen temperatures it begins to level off. This is because the deactivation rates do not allow increased laser energy. On the other hand, for the optimized lasers, the available specific energy continues to increase as  $\Delta T$  increases. This is because the optimizer has recognized the additional energy from the preheater and has adjusted the design to take advantage of it. As the nitrogen temperature was increased, the optimizer reduced the CO<sub>2</sub> concentration by selecting an alternate composition and thereby increased the amount of N<sub>2</sub> available for preheating. The reduction in flame temperature that occurred when the CO<sub>2</sub> concentration was reduced was compensated for by the increased N<sub>2</sub> temperature. Eventually, of course, the curves would begin to level off since there would be a point at which unacceptably low CO<sub>2</sub> concentrations (or low  $g_0$ ) would be obtained and no

Table 3 GDL performance results (optimal)

$P_o$ , atm	$\Delta T$ , °K	$T_o$ , °K	$\psi_{CO_2 OPT}$ (molar)	$\psi_{H_2O OPT}$ (molar)	$\epsilon_{OPT}$ , kJ/lb	$\epsilon_{NON-OPT}$ , kJ/lb
30	0	1846	0.156	0.015	17.1	11.4
	250	1868	0.143	0.017	18.5	14.7
	500	1925	0.133	0.017	20.1	17.8
	750	1949	0.117	0.017	22.0	20.5
	1000	1982	0.100	0.017	24.4	21.8
45	0	1861	0.158	0.014	15.7	10.7
	250	1878	0.145	0.013	17.1	13.9
	500	1892	0.129	0.013	18.6	16.9
	750	1935	0.116	0.013	20.5	19.6
	1000	1978	0.100	0.013	22.9	21.5
54	0	1860	0.158	0.013	14.9	10.4
	250	1848	0.141	0.010	16.3	13.4
	500	1887	0.129	0.011	17.9	16.4
	750	1927	0.115	0.012	19.8	19.2
	1000	1953	0.096	0.011	22.1	21.1
62	0	1848	0.156	0.014	14.2	10.1
	250	1837	0.140	0.009	15.7	13.1
	500	1875	0.127	0.010	17.3	16.0
	750	1912	0.113	0.010	19.2	18.7
	1000	1940	0.095	0.009	21.6	20.7

Fig. 1 Average available specific energy as a function of additional temperature of  $N_2$  (optimal and nonoptimal).

increase in the  $N_2$  concentration could be made. This tradeoff with  $CO_2$  concentration and temperature suggests that  $CO_2$  concentration is much more critical to the process than is temperature when preheating is used. The data of Table 3 show little change in  $T_o$ , but a large change in  $\psi_{CO_2}$ .

## Conclusions

From the data presented, it is evident that preheating can increase the available specific energy. In the case considered, and with no thermal losses,  $\epsilon$  was increased by up to 50%. Even more modest levels of preheating than the maximum assumed here (e.g.,  $\Delta T = 500$  K) can still produce a more than 30% improvement. Because no other laser parameter was changed, this effect was due solely to the increased stagnation temperature produced by the preheated nitrogen. The increase cannot be produced by simply changing the combustion conditions to obtain the high temperature, since excessive  $CO_2$  concentrations would be present. These results are consistent with the experimental trends discussed in Ref. 9, where an actual preheated laser is described.

## References

- <sup>1</sup>Gerry, E. T. "Gasdynamic Laser" *IEEE Spectrum*, Vol. 7, No. 51, Nov. 1970.
- <sup>2</sup>Anderson, J. D. and Harris, E., "Modern Advances in the Physics of Gasdynamic Lasers," AIAA Paper 72-143, San Diego, Calif., 1972.
- <sup>3</sup>Gerry, E. T., "Gasdynamic Lasers," presented at American Physical Society, Washington, D. C., 1970.
- <sup>4</sup>Wood, A. D., "Program for High Power Laser Techniques," Wright-Patterson Air Force Base, Ohio, Air Force Avionics Laboratory Rept. No. AFAL-TR-68-361, Vol. II.
- <sup>5</sup>Faires, V. M., *Therodynamics*, Fifth Ed., MacMillan Co., Toronto, 1970.
- <sup>6</sup>Vanderplaats, Garret N., "CONMIN-A Fortran Program for Constrained Function Minimization," NASA TM X-62,282, 1973.
- <sup>7</sup>Saunders, R. C. and Otten, L. J., "Optimized Gas Dynamic Lasers," Kirtland Air Force Base, New Mexico, Air Force Weapons Laboratory Rept. No. AFWL TR-74-344, 1975, pp. 291-299.
- <sup>8</sup>Avizonis, P. V., Dean, D. R., and Grotbeck, R., "Determination of Vibrational and Translation Temperature in Gas Dynamic Lasers," *Applied Physics Letters*, Vol. 23, No. 7, Oct. 1973, pp. 375-378.
- <sup>9</sup>Lundell, J. H., Otten, L. J., and Dickey, R. R., "The  $CO_2$  Gasdynamic Laser as a High-Intensity Radiation Facility," AIAA Paper 75-177, Pasadena, Calif., 1975.